REVIEW ARTICLE

Advances in the Application of Ultrasound Localization Microscopy in the Diagnosis of Andrological Diseases

Mingtai Wu[a], *Shijun Zhang*[a], *Li Xu*[a], *Lixin Jiang*[a,*]

[a] *Department of ultrasound, Ren Ji Hospital, Shanghai Jiao Tong University School of Medicine*

Received September 12, 2026; revision requested September 30, 2026; accepted December 5, 2026

Abstract: Male infertility, testicular tumors, and prostate cancer impose a substantial burden on male reproductive health and quality of life. Microcirculatory abnormalities are strongly correlated with the development and progression of these diseases; however, existing imaging modalities, constrained by their spatial resolution, are unable to visualize micrometer-scale microvascular structures in vivo. Ultrasound localization microscopy (ULM) combines imaging depth with high spatial resolution, surpassing the acoustic diffraction limit of conventional ultrasound and enabling the reconstruction of microvascular networks at the micrometer scale, while simultaneously providing multiple quantitative parameters. This article reviews the research progress of ULM in the diagnosis of andrological diseases and discusses the current challenges and future prospects.

Key words: Ultrasound localization microscopy; Male infertility; Testicular tumor; Prostate cancer

Advanced Ultrasound in Diagnosis and Therapy 2026; 04: 376-384 DOI: 10.26599/AUDT.2026.260036

Microcirculation is the terminal vascular network formed by blood flowing through arterioles, capillaries, and venules and serves as the structural basis of tissue perfusion and substance exchange [1]. The structural and functional status of the microcirculation directly affects tissue and organ metabolism and is broadly implicated in the initiation, progression, and prognosis of various diseases, including neurological disorders, metabolic diseases [2], and malignant tumors [3]. Sustained angiogenesis is essential for tumor growth, invasion, and metastasis [4]. In the field of andrology, testicular microcirculation is closely associated with spermatogenesis and seminiferous tubule function [5], whereas morphological and hemodynamic alterations of the prostatic microvasculature provide important information for the diagnosis of prostatic lesions. Therefore, accurate assessment of the structure and function of the microcirculation not only contributes to elucidating the pathophysiological mechanisms underlying these diseases but also holds significant clinical value for precise diagnosis, treatment optimization, and prognostic evaluation.

Ultrasound imaging has been widely used to visualize the vascular system owing to its safety, convenience, and low cost. However, conventional ultrasound imaging systems are constrained by the acoustic diffraction limit, and their spatial resolution is considerably coarser than the diameter of capillaries and other microvessels. Conventional color Doppler flow imaging can only depict blood flow signals from relatively large vessels within tissues and is unable to quantify microcirculatory perfusion characteristics; contrast-enhanced ultrasound (CEUS) can enhance the display of tissue perfusion, yet its spatial resolution is likewise limited by the diffraction limit, precluding precise assessment at the microvascular level and limiting the accurate evaluation of microvascular lesions in organs such as the testis and prostate.

Inspired by photoactivated localization microscopy (PALM) and stochastic optical reconstruction

* *Corresponding author: Department of ultrasound, Ren Ji Hospital, Shanghai Jiao Tong University School of Medicine, No. 160 Pujian Road, Pudong New Area, Shanghai 200127, China. (Lixin Jiang)*
e-mail: jinger_28@sina.com (LX J)

2576-2508/© AUDT 2026 • http://www.AUDT.org
This is an open-access article distributed under the terms of the Creative Commons Attribution 4.0 International license, which permits unrestricted use, distribution and reproduction in any medium provided that the original work is properly attributed.

microscopy (STORM), which overcame the optical diffraction limit via single-molecule localization [6,7], ultrasound localization microscopy (ULM) was developed. After intravenous injection of microbubble contrast agents, ULM detects, localizes and tracks individual microbubbles frame-by-frame, overcoming the conventional acoustic diffraction limit to reconstruct the microvascular network at a spatial resolution of 10 μm (typically 10-50 μm), while simultaneously quantifying hemodynamic parameters such as blood flow direction and velocity [8-10].

Compared with conventional ultrasound, ultrasound localization microscopy (ULM) markedly improves spatial resolution without significantly compromising imaging depth, can be performed noninvasively based on routine clinical CEUS examinations, and provides a new tool for the in vivo assessment of microcirculatory structure and function [11] (Table 1). To date, this technique has been applied to the diagnosis of diseases of the liver [12], kidney [13], breast [14], brain [15], and heart [16], and its application in andrological diseases has also demonstrated promising prospects. This review comprehensively summarizes the current applications of this emerging technique in andrological diseases and discusses the remaining challenges and future directions.

Assessment of Testicular Microcirculation

Classification of azoospermia

The World Health Organization notes that infertility represents a major global reproductive health concern among couples of reproductive age. Its prevalence ranges from 10% to 20%, and male-related causes are responsible for 30%-50% of these cases [17-19]. As a severe subtype of male infertility, azoospermia affects 10%-20% of infertile males and is clinically categorized into obstructive azoospermia (OA) and non-obstructive azoospermia (NOA). OA, which accounts for nearly 40% of azoospermia cases, is characterized by normal testicular spermatogenesis accompanied by obstruction of the reproductive tract and can be treated surgically to relieve the obstruction; NOA results from impaired spermatogenesis within the testis itself, although focal spermatogenic regions may persist in the testes of some patients, allowing surgical sperm retrieval. Because the treatment strategies for these two conditions differ substantially, accurate classification is essential for individualized diagnosis and treatment planning [20,21]. Currently, clinical methods for distinguishing NOA from OA remain limited. Although testicular biopsy remains the reference standard for azoospermia subtyping and

Table 1 Comparison of different diagnostic methods for andrological diseases

Dimension	Testicular biopsy	Prostate mpMRI	CEUS	ULM
Diagnostic performance	Histopathological gold standard with the highest accuracy	Based on PI-RADS scoring, high sensitivity but moderate specificity for detecting clinically significant prostate cancer	Real-time qualitative/semi-quantitative assessment of tissue perfusion; moderate value in differentiating benign from malignant lesions	Mean vessel diameter yielded AUCs of 0.920 and 0.952 in discriminating non-obstructive from obstructive oligoasthenozoospermia and azoospermia, respectively. [24]; combined FSH + mean vessel diameter for NOA vs. OA: AUC 0.968, accuracy 92.6% [25]; AUC 0.88-0.91 for identifying HH [26]; prostate cancer foci detection rate 94.1% [27]; AUC 0.832 for distinguishing benign vs. malignant prostatic lesions [28]
Invasiveness/safety	Invasive; risks include testicular parenchymal injury and impaired fertility potential [22,23]	Non-invasive (intravenous contrast; contraindicated in renal insufficiency)	Non-invasive (intravenous microbubble contrast; adverse reactions are rare)	Non-invasive (intravenous microbubble contrast; adverse reactions are rare)
Cost	High	High	Moderate	Moderate
Clinical availability	High (routine in urological practice)	Moderate (high equipment cost, long waiting lists)	High (available in most hospitals)	Low (equipment not yet widely disseminated; multicenter evidence still accumulating)
Advantages	Provides direct histopathological evidence	High spatial resolution; multiparametric assessment	Real-time, repeatable, ionizing-radiation-free	Repeatable, dynamic, high-resolution; quantitative microvascular assessment
Limitations	Sampling error, complications, non-repeatable; cannot dynamically assess microcirculation	False negatives, high cost, limited accessibility, contrast contraindications, and metallic implants	Resolution constrained by the acoustic diffraction limit; cannot visualize microvessels	Long acquisition/post-processing time, susceptible to respiratory and cardiac motion, dependent on microbubble concentration, insufficient large-sample clinical validation

Abbreviations: CEUS, contrast-enhanced ultrasound; FSH, follicle-stimulating hormone; HH, hypogonadotropic hypogonadism; mpMRI, multiparametric magnetic resonance imaging; NOA/OA, non-obstructive/obstructive azoospermia; PI-RADS, Prostate Imaging Reporting and Data System; ULM, ultrasound localization microscopy.

yields comprehensive histological data, this procedure is invasive and bears risks including testicular parenchymal damage and impaired fertility potential [22,23] (Table 1); serum hormone testing, by contrast, is affected by multiple factors and has low diagnostic specificity.

With respect to conventional ultrasound techniques, grayscale ultrasound can indirectly reflect spermatogenic function on the basis of testicular volume and testicular parenchymal echogenicity [29]. Color Doppler ultrasound (CDUS) can assess testicular blood perfusion; Herwig et al. [30] found that regions with abundant blood supply exhibited the best sperm quality and the highest sperm counts, yet CDUS can only depict the distribution of large vessels and cannot identify microvascular regions with rich perfusion [31]. CEUS can display testicular microvascular perfusion. In a study of 95 patients with NOA, Zhang et al. [32] demonstrated that the success rate of microdissection testicular sperm extraction (micro-TESE) within contrast-enhanced areas was 66.3%, which was markedly higher than that observed in low-perfusion regions (32.6%) and conventional regions (47.3%). Subsequent studies [33,34] also further confirmed that quantitative CEUS parameters can predict the success rate of sperm retrieval. Superb microvascular imaging (SMI) can clearly display low-velocity blood flow signals and microvascular distribution within the testis, reflecting intratesticular microvascular perfusion. Using this technique, Liu et al. [35] found that high-density microvessels were correlated with foci of spermatogenesis within the testes of patients with NOA, and that the sperm retrieval rate in regions with abundant blood flow was significantly higher than that in conventional and sparse regions. Furthermore, testicular ultrasound microvascular density (UMVD) and ultrasound-estimated testicular volume (UVE) can predict micro-TESE outcomes among patients with NOA; the group with successful sperm retrieval exhibited markedly higher UMVD and UVE values relative to patients with failed retrieval [36]. However, none of the aforementioned techniques can visualize and quantify the microvasculature at the capillary level, nor can they systematically elucidate the intrinsic relationship between testicular microcirculation and spermatogenic function.

To address this clinical limitation, Li et al. [24] achieved non-invasive super-resolution imaging of human testicular microcirculation in a multicenter study, resolving testicular vessels separated by as little as 81 μm, with spatial resolution superior to that of existing imaging modalities. The study enrolled 76 infertile patients and 15 healthy controls and found that mean vessel diameter yielded area under the curve (AUC) values of 0.920 and 0.952 in differentiating non-obstructive from obstructive causes of oligoasthenozoospermia and azoospermia, respectively, demonstrating favorable discriminative performance and providing a new imaging reference for the non-invasive classification of male infertility.

Furthermore, Li et al. [25] enrolled 94 patients with azoospermia (36 cases of NOA and 58 cases of OA), and used ULM to quantitatively extract five parameters—flow velocity, tortuosity, diameter, fractal number and vessel density—to characterize testicular microcirculation, and analyzed their associations with spermatogenesis-related clinical indices. The results showed that the mean vessel diameter, vessel density, and fractal number were significantly higher in the OA group than in the NOA group, whereas there were no significant differences between the two groups in blood flow velocity and vessel tortuosity. Furthermore, based on ULM blood flow velocity data, the authors constructed pressure distribution maps of the testicular microvasculature and found that NOA was characterized by low blood flow density, uneven pressure distribution, and focal hypoperfusion, consistent with the pathological features of impaired spermatogenesis. In contrast, OA exhibited higher vessel density and uniform blood flow distribution, manifesting as a more homogeneous pressure distribution with compensatory angiogenesis. These findings visually demonstrated the microcirculatory differences between the two types of azoospermia from a hemodynamic perspective, providing imaging evidence for understanding the pathophysiological mechanisms of azoospermia. Meanwhile, significant associations were also observed between the testicular microcirculatory parameters measured by ULM and clinical indicators of spermatogenic function, including follicle-stimulating hormone (FSH) and luteinizing hormone (LH). Specifically, FSH was negatively correlated with mean vessel diameter, suggesting that elevated FSH may reflect structural impairment of testicular microcirculation and further corroborating the intrinsic association between microvascular status and testicular endocrine and spermatogenic function. Based on these findings, the authors constructed a logistic regression diagnostic model combining FSH with mean vessel diameter. The model achieved an AUC of 0.968 in differentiating NOA from OA, with an overall diagnostic accuracy of 92.6%, demonstrating significantly better diagnostic performance than either parameter alone and providing a new imaging reference for the noninvasive differentiation of NOA and OA. However, this study was a single-center retrospective cross-sectional study that was limited to two-dimensional imaging.

In an experimental study, Ye et al. [37] established a classification system combining ULM with multi-omics

清華大學出版社 Tsinghua University Press | SciOpen

analysis. By achieving quantitative in vivo imaging of the testicular microvasculature, they revealed etiology-specific microvascular phenotypes of azoospermia: NOA mouse models (busulfan-treated and *Pnldc1-KO*) exhibited fragmented vascular networks and hypoperfusion, with reduced diameter of large intratesticular vessels; OA mouse models exhibited increased vessel density, increased mean vessel diameter, and increased mean blood flow velocity. Through transcriptomics and metabolomics analysis, researchers linked the imaging phenotypes mentioned above to molecular mechanisms such as angiogenesis and extracellular matrix remodeling, revealing the connections between imaging phenotypes, molecular mechanisms, and histology. This systematically elucidated the intrinsic association between testicular microcirculation and spermatogenesis, deepened the understanding of the microcirculatory mechanisms underlying the pathogenesis of azoospermia, and demonstrated the utility of ULM in distinguishing OA from NOA. These findings further underscore the potential of ULM to optimize assisted reproductive strategies and guide sperm retrieval, pending confirmation in human studies.

Collectively, quantitative ULM parameters enable in vivo differentiation of the characteristic microvascular phenotypes between OA and NOA, providing imaging evidence for elucidating the microcirculatory mechanisms underlying azoospermia and guiding clinical sperm retrieval.

Hypogonadism

Hypogonadotropic hypogonadism (HH) results from dysfunction of the hypothalamic–pituitary axis, which leads to insufficient secretion of gonadotropins (FSH and LH) and subsequently causes testicular hypoplasia, testosterone deficiency, and impaired spermatogenesis. It constitutes an important etiology of male infertility [38,39]. Unlike most etiologies of male infertility, HH is among the few conditions in which fertility can be reversed by pharmacological treatment, and most patients can regain fertility after medical therapy [40,41]. Early identification of HH and regular monitoring of endocrine therapy are therefore crucial for improving reproductive outcomes. However, the diagnosis and therapeutic evaluation of HH currently rely mainly on indirect indicators, such as sex hormone levels and testicular volume, lacking direct visualization of the structural basis of testicular function. Testicular microcirculation is the structural basis of testicular function. Using CEUS, Carlomagno et al. [42] demonstrated that testicular perfusion dynamics were significantly slowed in patients with Klinefelter syndrome, and that reduced venous blood flow could independently predict circulating testosterone levels, suggesting a close association between microcirculatory status and testicular endocrine function. However, conventional ultrasound is unable to precisely quantify microvascular structures; therefore, more sensitive imaging modalities are urgently needed for the direct evaluation of testicular microcirculation.

ULM can overcome the aforementioned limitations. Papanikolaou et al. [26] conducted a prospective case-control study using hypogonadotropic hypogonadism (HH) as a disease model of impaired testicular function and validated the translational value of ULM in both humans and rats. The study demonstrated that in patients with HH, testicular microvascular density, vessel diameter, vascular area, and blood flow-related indices were significantly reduced compared with healthy controls, whereas vascular tortuosity was increased. These parameters were significantly correlated with serum testosterone and inhibin B levels, and microvascular impairment was more pronounced in patients with azoospermia. Receiver operating characteristic (ROC) curve analysis indicated that ULM exhibited good discriminative performance for HH (AUC 0.88-0.91). Gonadotropin therapy significantly improved microvascular density and vessel diameter in patients with HH, whereas testosterone replacement therapy alone failed to reverse these alterations. Longitudinal follow-up demonstrated that ULM parameters improved promptly following gonadotropin therapy, earlier than traditional markers such as testicular volume and inhibin B. A rat model of pubertal arrest further confirmed that gonadal hormone suppression could induce testicular microvascular remodeling. Collectively, this study not only confirmed the association between microcirculatory blood flow and testicular spermatogenic and endocrine function, but also indicated that ULM parameters hold promise as sensitive biomarkers for assessing testicular functional status and therapeutic response, facilitating patient stratification and early prediction of treatment efficacy.

Testicular tumors

Testicular germ cell tumors represent the most prevalent solid malignancies in men aged 15-40 years, with an increasing incidence worldwide [43,44]. Tumor angiogenesis is a key driver of tumor proliferation, invasion, and distant metastasis, and abnormalities of tumor neovascularization are highly correlated with tumor biological behavior. Studies have demonstrated that tumor tissues highly express pro-angiogenic factors such as vascular endothelial growth factor (VEGF), which can induce the formation of abnormal vascular networks characterized by increased microvascular density and tortuous, disordered vessel courses. Furthermore,

microvascular morphological features are closely associated with malignant pathological phenotypes such as vascular invasion, and can serve as an indirect indicator of the malignant biological behavior [45,46].

As the preferred imaging technique for testicular neoplasms, scrotal ultrasound achieves high sensitivity for identifying testicular lesions [47,48]. However, conventional ultrasound and CEUS can only reflect the overall perfusion level of the testis, whereas ULM enables visualization of the microvascular network and provides potential imaging references for the classification and malignant risk assessment of testicular tumors (Fig. 1-2).

In 2024, Lock et al. [49] acquired CEUS data from patients with pathologically confirmed seminoma after surgery, performed ULM postprocessing, reconstructed vascular trajectory maps and blood flow velocity maps, and compared these images with CEUS maximum intensity projection (MIP) images.

The results demonstrated that the ULM images clearly delineated the morphology of intratumoral microvascular networks and more intuitively revealed high- and low-perfusion regions. The ULM velocity map measured an average microbubble flow velocity of approximately 102 μm/s within the tumor region, and the large vessels showing enhancement on MIP images also exhibited higher flow velocities on the ULM velocity map. By characterizing the morphological and hemodynamic features of tumor microvasculature, this technique holds promise as a novel tool for preoperative assessment, treatment response monitoring, and identification of vascular-derived biomarkers, and may be further extended to microvascular imaging of other tumors.

Assessment of Microcirculation in Prostate Diseases

As one of the most frequently occurring malignant neoplasms in the male genitourinary system, prostate

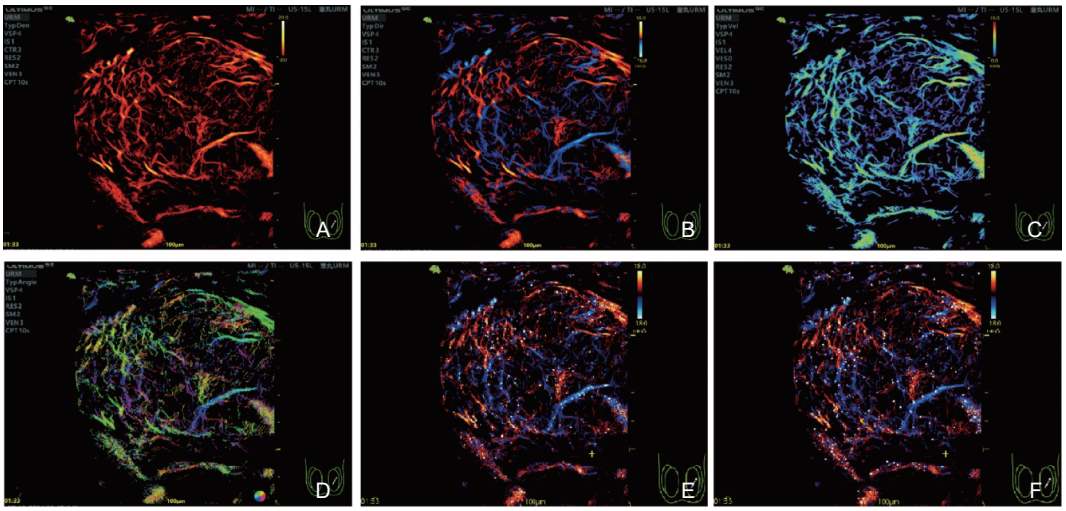


Figure 1 ULM images of a 36-year-old patient with testicular seminoma. (A) Microvascular density map, reflecting local relative blood volume; (B) Microvascular blood flow direction map, reflecting blood supply characteristics; (C) Microvascular blood flow velocity map; (D) Microbubble flow angle map inside microvessels, a reference indicator of the degree of blood flow disorder; (E, F) Microbubble flow images at different times, reflecting the spatiotemporal evolution of blood perfusion. ULM, ultrasound localization microscopy.

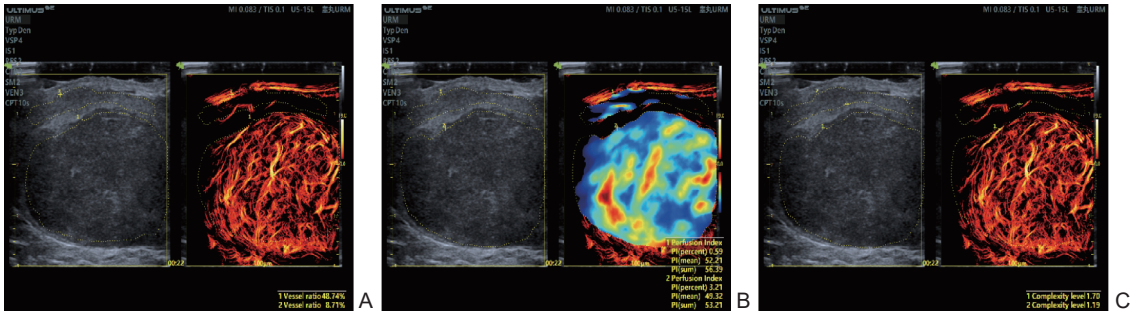


Figure 2 ULM parameter analysis images of a 29-year-old patient with a left testicular seminoma. (A) Vessel ratio in the tumor region is significantly higher than in normal testicular tissue (48.74% vs 8.71%), indicating a richer blood supply in the tumor area; (B) Perfusion index (Percent) in the tumor region is increased compared to normal testicular tissue (3.21 vs 0.59); (C) Complexity level in the tumor region is significantly higher than in normal testicular tissue (1.70 vs 1.19). Vascular ratio and perfusion index reflect the spatial proportion of tumor microvessels and local blood volume, respectively, representing the quantitative dimension of angiogenesis. Complexity level quantifies the tortuosity, branching, and disorganized arrangement of the vascular network, corresponding to its structural dimension. In the present case, these parameters were concurrently elevated within the tumor region, consistent with the pathological manifestations of seminoma. ULM, ultrasound localization microscopy.

清華大學出版社 Tsinghua University Press | SciOpen

cancer exhibits a sustained increase in incidence attributable to population aging. Most patients are already at a locally advanced or metastatic stage at initial diagnosis, with an overall poor prognosis; hence, early and accurate identification of prostate cancer plays a vital role in informing clinical treatment decisions and improving patient prognosis [50,51]. Tumor angiogenesis constitutes the pathological basis of prostate cancer progression, invasion, and metastasis. Tumor tissues exhibit increased microvascular density and distorted, disordered vascular morphology, and these microvascular features are closely correlated with Gleason grade and malignant tumor behavior [52,53].

Butler et al. [54] performed conventional transrectal CEUS acquisition in 14 patients with suspected prostate cancer, encompassing 54 imaging planes in total, and described the ULM microvascular patterns of prostate cancer. The results showed that 10 biopsy-confirmed cancerous imaging planes with a Gleason score $\geq$ 7 exhibited characteristic microvascular heterogeneity: 7 planes showed focal high-velocity, high-flow regions, and 6 planes showed coexistence of avascular and high-flow regions, some planes exhibited both features, cancer-negative planes, in contrast, showed relatively homogeneous blood flow distribution with low flow velocities. Quantitative analysis revealed that the mean flow velocity of high-flow cancerous lesions was significantly higher than that of non-cancerous regions in the same plane, whereas some cancerous lesions were predominantly characterized by avascular regions. These findings suggest that the spatial heterogeneity of the microvasculature revealed by ULM, particularly the distribution patterns of high-flow and avascular regions, may provide a novel imaging reference for localizing clinically significant prostate cancer, thereby compensating for the limitation of multiparametric MRI (mpMRI) in visualizing certain lesions.

Subsequently, Butler et al. [27] used whole-mount pathology after radical prostatectomy as the reference standard and identified 16 of 17 confirmed cancerous foci in the initial subgroup (detection rate 94.1%), with the lesions characterized by higher flow velocity, higher blood flow, and relatively wider vessels. The study also systematically characterized the ULM features of benign structures within the prostate: benign prostatic hyperplasia (BPH) nodules exhibited a pattern of central avascular cystic regions, peripheral low-flow bands, and high-capacity large vessels; cystically dilated glands were nearly avascular; and periurethral vessels appeared as symmetric, continuous, well-defined high-flow conduits. In addition, cancerous foci in the posterior peripheral zone showed the highest conspicuity, whereas those in the transition zone and anterior region exhibited poor contrast due to the relatively rich background blood supply. Integrating multiparametric ULM features while accounting for anatomical zone differences holds promise for the localization of prostate cancer and the differentiation between benign and malignant lesions.

Huang et al. [28] conducted a clinical study of ULM with a relatively large sample size, enrolling 127 patients with prostatic lesions (78 benign and 49 malignant), and systematically investigated the diagnostic value of ULM in distinguishing benign from malignant prostatic lesions, using biopsy pathology as the gold standard. The study found that microvascular density, vessel diameter, flow velocity, tortuosity, and fractal number were all markedly higher in malignant lesions relative to benign lesions, with vessel diameter exhibiting the best diagnostic performance (AUC 0.832, sensitivity 85.7%, specificity 63.6%). Furthermore, certain time-intensity curve parameters of CEUS also showed differences between the two groups.

Zhao et al. [55] enrolled men scheduled for prostate biopsy in whom transrectal ultrasound revealed no focal nodules. These patients underwent transrectal CEUS with acquisition of ULM images, and the quantitative microvascular features were compared between patients with diffuse prostate cancer and those with prostatic hyperplasia. The results showed that microvascular complexity, mean blood flow velocity, mean perfusion index, mean microvascular diameter, and entropy in both the inner and outer prostate glands were significantly higher in the prostate cancer group than in the prostatic hyperplasia group, with statistically significant differences.

Collectively, these studies demonstrate that ULM can noninvasively quantify parameters such as microcirculatory perfusion, microvascular density, and vascular morphology, reflecting alterations in the prostate tumor microenvironment, and may facilitate the discrimination between benign and malignant lesions as well as the localization of prostate cancer, thereby providing objective imaging evidence for the precise diagnosis and treatment of prostate cancer. However, current prostate ULM examinations are predominantly acquired via the transrectal approach, with several inherent limitations. First, transrectal probes frequently induce substantial rectal irritation and tenesmus. Second, the technique suffers from operator dependence: the compression force, angle and stability of the probe against the rectal wall may alter the trajectory and flow velocity of prostatic microvessels. Variations in immobilization maneuvers and region-of-interest (ROI) delineation habits among different operators can also lead to discrepancies in results.

Potential Applications in Other Andrological Diseases

Beyond the aforementioned diseases, ULM also holds potential value in other andrological conditions. Varicocele, one of the common causes of male infertility, can lead to abnormal testicular microcirculatory perfusion. ULM holds promise for the quantitative assessment of testicular microcirculatory damage caused by varicocele and for monitoring hemodynamic recovery before and after surgical intervention; however, to date no ULM studies have been reported in the field of varicocele, and the only available evidence for erectile dysfunction (ED) is derived from rat models, with clinical human data still relatively scarce.

ED is closely associated with penile vascular endothelial function and microcirculatory perfusion. Yang et al. [56] designed a liposomal microbubble co-loaded with sildenafil (a phosphodiesterase type 5 [PDE5] inhibitor) and nitric oxide (NO) (Sil-NO-MBs). After tail vein injection, ultrasound-targeted microbubble destruction (UTMD) was applied to achieve localized and precise release of the drug and gas in a rat model of cavernous nerve injury. Using ULM imaging, the authors visualized and quantified the microvascular network of the penile corpus cavernosum, providing imaging evidence for the improvement of microcirculation by UTMD. The results showed that Sil-NO-MBs combined with UTMD significantly improved penile microvascular perfusion, alleviated cavernous fibrosis, and reversed structural remodeling, ultimately promoting the recovery of erectile function. This study expanded the scope of ULM application in the assessment of erectile dysfunction and laid a foundation for subsequent basic and clinical research.

Challenges and Prospects

Despite the promising potential of ULM in diagnosing andrological diseases, its clinical translation still faces multiple challenges.

Technical challenges: First, there is an inherent trade-off between acquisition time and frame rate. Sufficient microbubble localizations must be accumulated. High-frame-rate systems can finish acquisition within seconds, but such clinical devices are not yet widely available. On conventional systems, acquisition takes seconds to minutes, which raises the risk of motion artifacts. Second, ULM relies on exogenous contrast agents, making it difficult to precisely control microbubble blood concentration, and safety related to contrast use must be considered. Third, the testes are superficial and highly mobile. During transrectal prostate examination, probe stability is limited. Both tissue movement and probe displacement cause inter-frame displacement, which blurs the reconstructed image. In addition, ULM modules have not been integrated into most clinical CEUS systems. Current studies largely depend on off-line reconstruction. Constrained by immature hardware integration and limited real-time processing power, few commercial products are available. This further slows clinical adoption.

Methodological challenges: First, ULM remains an experimental technique. Most clinical studies on ULM in andrological diseases are single-center, small-sample, retrospective, or cross-sectional exploratory studies. Except for Li et al. [24], who reported multi-center enrollment, all diagnostic models were built and internally validated in single-center cohorts. The diagnostic thresholds have not been externally validated in large, prospective, multi-center studies across different populations and devices. At present, ULM cannot replace biopsy or routine clinical imaging. Second, ultrasound scanners, contrast protocols, and post-processing pipelines differ across studies. This heterogeneity makes it impossible to directly compare ULM parameters and diagnostic performance between studies [57]. Third, few studies report the reproducibility of ULM quantitative parameters, including intra-reader and inter-reader agreement. This is another barrier to clinical translation. Therefore, large-scale prospective multi-center studies are urgently needed. They should establish standardized acquisition and post-processing protocols, reference ranges for quantitative parameters, and diagnostic thresholds.

Future directions include: (1) three-dimensional ULM for the reconstruction of organ microvascular networks and multidimensional motion correction; (2) multimodal fusion of ULM with MRI and photoacoustic imaging to provide more comprehensive anatomical and functional information; (3) ultrasound molecular imaging based on targeted microbubbles for in vivo visualization and detection of disease-specific biomarkers; (4) automated image analysis and diagnostic decision support assisted by artificial intelligence and deep learning algorithms; (5) extension from diagnosis alone to treatment monitoring, such as dynamic monitoring of therapeutic efficacy in male infertility and early response assessment of tumor anti-angiogenic therapy; and (6) ultrasound microvascular radiomics: by constructing a microvascular characteristic spectrum, it is possible to achieve a more precise and personalized assessment of microvascular conditions. However, in practical applications, factors such as standardized feature selection and the risk of overfitting need to be taken into consideration [58].

Conclusions

By overcoming the conventional acoustic diffraction limit, ULM enables in vivo visualization of microvessels at the micrometer scale and quantitative hemodynamic assessment, providing a new imaging perspective for the diagnosis of andrological diseases. However, it should be noted that current research still has some limitations, and its clinical diagnostic performance remains to be further validated. With ongoing advances in imaging speed, algorithm optimization, three-dimensional imaging, device integration, and microvasculomics, ULM is expected to gain increasingly widespread adoption in routine clinical andrological practice.

Acknowledgment

Not applicable.

Authors' Contributions

Mingtai Wu completed the writing of the article. Shijun Zhang and Li Xu completed the revisions. Lixin Jiang designed the idea of the review and completed the revisions. All authors participated in revising the manuscript and have read and approved the final submitted version.

Funding

This work was supported by the Shanghai Oriental Elite Plan Outstanding Project, National Natural Science Foundation of China (82572225), Medical New Technology Research and Transformation Seed Program of Shanghai Municipal Health Commission (2025ZZ1007), Key Discipline Construction Project of Shanghai Health System in 2024 (2024ZDXK0059), Key Discipline Construction Project of Jiading District Health System (XK202403).

Data Availability

Not applicable.

Declarations

Ethics approval and consent to participate

Not applicable.

Conflict of interest

The authors declare no conflicts of interest.

Consent for publication

Written informed consent was obtained from the patients for publication of Figures 1 and 2.

References

[1] Guven G, Hilty MP, Ince C. Microcirculation: physiology, pathophysiology, and clinical application. Blood Purif 2020;49:143-150.
[2] Yuan Y, Dong M, Wen S, Yuan X, Zhou L. Retinal microcirculation: a window into systemic circulation and metabolic disease. Exp Eye Res 2024;242:109885.
[3] Alameddine RS, Hamieh L, Shamseddine A. From sprouting angiogenesis to erythrocytes generation by cancer stem cells: evolving concepts in tumor microcirculation. Biomed Res Int 2014;2014:986768.
[4] Sharma S, Sharma MC, Sarkar C. Morphology of angiogenesis in human cancer: a conceptual overview, histoprognostic perspective and significance of neoangiogenesis. Histopathology 2005;46:481-489.
[5] Ergün S, Kilic N, Harneit S, Paust HJ, Ungefroren H, Mukhopadhyay A, et al. Microcirculation and the vascular control of the testis. Adv Exp Med Biol 1997;424:163-180.
[6] Betzig E, Patterson GH, Sougrat R, Lindwasser OW, Olenych S, Bonifacino JS, et al. Imaging intracellular fluorescent proteins at nanometer resolution. Science 2006;313:1642-1645.
[7] Rust MJ, Bates M, Zhuang X. Sub-diffraction-limit imaging by stochastic optical reconstruction microscopy (STORM). Nat Methods 2006;3:793-795.
[8] Christensen-Jeffries K, Couture O, Dayton PA, Eldar YC, Hynynen K, Kiessling F, et al. Super-resolution ultrasound imaging. Ultrasound Med Biol 2020;46:865-891.
[9] Dencks S, Schmitz G. Ultrasound localization microscopy. Z Med Phys 2023;33:292-308.
[10] Yi HM, Lowerison MR, Song PF, Zhang W. A review of clinical applications for super-resolution ultrasound localization microscopy. Curr Med Sci 2022;42:1-16.
[11] Chen Q, Song H, Yu J, Kim K. Current development and applications of super-resolution ultrasound imaging. Sensors (Basel) 2021;21:2417.
[12] Zeng QQ, An SZ, Chen CN, Wang Z, Liu JC, Wan MX, et al. Focal liver lesions: multiparametric microvasculature characterization via super-resolution ultrasound imaging. Eur Radiol Exp 2024;8:138.
[13] Huang C, Abdelfattah A, DeRuiter RM, Zhang N, Knoll KM, Petersen KE, et al. Ultrasound localization microscopy to assess the intrarenal microvasculature in autosomal dominant polycystic kidney disease. J Am Soc Nephrol 2026;37:1221-1236.
[14] Li J, Wei C, Ying T, Liu Y, Wang R, Li M, et al. Differentiation of benign and malignant breast lesions by ultrasound localization microscopy. Insights Imaging 2025;16:128.
[15] Li M, Wang W, Su Z, Wu J, Yang Y, Wang L, et al. Clinically translatable ultrasound localization microscopy reveals cerebrovascular remodelling and prognosis in patients with traumatic brain injury. Nat Biomed Eng. Published online June 17, 2026.
[16] Huang B, Tonko J, Yan J, Smith CAB, Gvinianidze L, Toulemonde M, et al. Multiphase myocardial microvascular flow dynamics revealed by transthoracic ultrasound localization microscopy in HCM and non-HCM patients. JACC Cardiovasc Imaging 2025;18:1276-1278.
[17] Inhorn MC, Patrizio P. Infertility around the globe: new thinking on gender, reproductive technologies and global movements in the 21st century. Hum Reprod Update 2015;21:411-426.
[18] Agarwal A, Mulgund A, Hamada A, Chyatte MR. A unique view on male infertility around the globe. Reprod Biol Endocrinol 2015;13:37.
[19] Agarwal A, Baskaran S, Parekh N, Cho CL, Henkel R, Vij S, et al. Male infertility. Lancet 2021;397:319-333.
[20] Wosnitzer M, Goldstein M, Hardy MP. Review of azoospermia. Spermatogenesis 2014;4:e28218.
[21] Practice Committee of the American Society for Reproductive Medicine. Management of nonobstructive azoospermia: a committee opinion. Fertil Steril 2018;110:1239-1245.
[22] Esteves SC, Miyaoka R, Agarwal A. Sperm retrieval techniques for assisted reproduction. Int Braz J Urol 2011;37:570-583.

[23] Eliveld J, van Wely M, Meißner A, Repping S, van der Veen F, van Pelt AMM. The risk of TESE-induced hypogonadism: a systematic review and meta-analysis. Hum Reprod Update 2018;24:442-454.
[24] Li M, Chen L, Yan J, Jayasena CN, Liu Z, Li J, et al. Super-resolution ultrasound localization microscopy for the non-invasive imaging of human testicular microcirculation and its differential diagnosis role in male infertility. View 2024;5:20230093.
[25] Li M, Zhang X, Yan J, Shu H, Li Z, Ye C, et al. Non-invasive ultrasound localization microscopy (ULM) in azoospermia: connecting testicular microcirculation to spermatogenic functions. Theranostics 2024;14:4967-4982.
[26] Papanikolaou N, Yan J, Huang B, Davies R, Dunsterville C, De Silva NL, et al. Ultrasound localisation microscopy tracks testicular microvascular adaptations to endocrine function in male infertility. EBioMedicine 2026;129:106333.
[27] Butler MB, Papageorgiou G, Gallagher K, Arthur L, Keanie J, Grigorescu R, et al. Microvascular features of the prostate using super-resolution ultrasound. In: 2025 IEEE International Ultrasonics Symposium (IUS). Utrecht, Netherlands: IEEE 2025:1-3.
[28] Huang X, Ye H, Hu Y, Lei Y, Tian Y, Huang X, et al. Ultrasound super-resolution imaging for non-invasive assessment of microvessel in prostate lesion. Cancer Imaging 2025;25:1.
[29] Spaggiari G, M Granata AR, Santi D. Testicular ultrasound inhomogeneity is an informative parameter for fertility evaluation. Asian J Androl 2020;22:302-308.
[30] Herwig R, Tosun K, Schuster A, Rehder P, Glodny B, Wildt L, et al. Tissue perfusion-controlled guided biopsies are essential for the outcome of testicular sperm extraction. Fertil Steril 2007;87:1071-1076.
[31] Herwig R, Tosun K, Pinggera GM, Soelder E, Moeller KT, Pallwein L, et al. Tissue perfusion essential for spermatogenesis and outcome of testicular sperm extraction (TESE) for assisted reproduction. J Assist Reprod Genet 2004;21:175-180.
[32] Zhang SJ, Du J, Lü RH, Tian RH, Li FH. Application of contrast enhanced ultrasound in assessing the testicular spermatogenesis of nonobstructive azoospermia patients. J Shanghai Jiao Tong Univ (Med Sci) 2017;37:1368-1371. (in Chinese).
[33] Zhang S, Du J, Tian R, Xie S, Li F, Li Z. Assessment of the use of contrast enhanced ultrasound in guiding microdissection testicular sperm extraction in nonobstructive azoospermia. BMC Urol 2018;18:48.
[34] Xue H, Wang SY, Cui LG, Hong K. Can contrast-enhanced ultrasound increase or predict the success rate of testicular sperm aspiration in patients with azoospermia? AJR Am J Roentgenol 2019;212:1054-1059.
[35] Liu TM, Zheng S, Chen R, Xiao B. Application value of multimodal ultrasound technology in microdissection testicular sperm extraction for idiopathic non-obstructive azoospermia. J Hubei Univ Med 2024;43:152-156,178. (in Chinese).
[36] Cui J, Fu W, Song Y. Testicular ultrasonic microvascular density in assessing spermatogenesis and predicting successful sperm retrieval. Quant Imaging Med Surg 2024;14:4903-4912.
[37] Ye C, Lu Q, Yang K, Li M, Feng C, Chen L. Integrated ultrasound localization microscopy and multi-omics for mechanism-driven stratification of azoospermia. Am J Mens Health 2026;20:15579883261468072.
[38] Boehm U, Bouloux PM, Dattani MT, de Roux N, Dodé C, Dunkel L, et al. Expert consensus document: European consensus statement on congenital hypogonadotropic hypogonadism—pathogenesis, diagnosis and treatment. Nat Rev Endocrinol 2015;11:547-564.
[39] Young J, Xu C, Papadakis GE, Acierno JS, Maione L, Hietamäki J, et al. Clinical management of congenital hypogonadotropic hypogonadism. Endocr Rev 2019;40:669-710.
[40] Fraietta R, Zylberstejn DS, Esteves SC. Hypogonadotropic hypogonadism revisited. Clinics (Sao Paulo) 2013;68 Suppl 1:81-88.
[41] Kathrins M, Niederberger C. Diagnosis and treatment of infertility-related male hormonal dysfunction. Nat Rev Urol 2016;13:309-323.
[42] Carlomagno F, Pozza C, Tenuta M, Pofi R, Tarani L, Sesti F, et al. Testicular microvascular flow is altered in Klinefelter syndrome and predicts circulating testosterone. J Clin Endocrinol Metab 2022;107:e236-e245.
[43] McHugh DJ, Gleeson JP, Feldman DR. Testicular cancer in 2023: current status and recent progress. CA Cancer J Clin 2024;74:167-186.
[44] Znaor A, Lortet-Tieulent J, Jemal A, Bray F. International variations and trends in testicular cancer incidence and mortality. Eur Urol 2014;65:1095-1106.
[45] Jones A, Fujiyama C, Turner K, Fuggle S, Cranston D, Turley H, et al. Angiogenesis and lymphangiogenesis in stage 1 germ cell tumours of the testis. BJU Int 2000;86:80-86.
[46] Viglietto G, Romano A, Maglione D, Rambaldi M, Paoletti I, Lago CT, et al. Neovascularization in human germ cell tumors correlates with a marked increase in the expression of the vascular endothelial growth factor but not the placenta-derived growth factor. Oncogene 1996;13:577-587.
[47] Huang DY, Sidhu PS. Focal testicular lesions: colour Doppler ultrasound, contrast-enhanced ultrasound and tissue elastography as adjuvants to the diagnosis. Br J Radiol 2012;85 Spec No 1:S41-S53.
[48] Saidian A, Bagrodia A. Imaging techniques to differentiate benign testicular masses from germ cell tumors. Curr Urol Rep 2023;24:451-454.
[49] Lock D, Parra Raad J, Huang DY, Fang C, Sidhu PS, Tang M, et al. Mapping testicular tumor microvasculature with super-resolution ultrasound imaging. In: 2024 IEEE Ultrasonics, Ferroelectrics, and Frequency Control Joint Symposium (UFFC-JS). Taipei, Taiwan: IEEE 2024:1-4.
[50] Gan Y, Zhou H, Feng P, Gao H, Li R, Wang S. Global trends and regional variations in PCa burden: a focus on China's rapid growth. Urol Oncol 2025;43:526.e17-526.e31.
[51] Kim JK, Park MU, Lee D, Kim HJ, Shin T, Shim M, et al. Sustained PSA screening is associated with downstaging and improved survival in prostate cancer: a 12-year Korean cohort study. BMC Cancer 2025;25:1462.
[52] Weidner N, Carroll PR, Flax J, Blumenfeld W, Folkman J. Tumor angiogenesis correlates with metastasis in invasive prostate carcinoma. Am J Pathol 1993;143:401-409.
[53] Grizzi F, Hegazi MAAA, Zanoni M, Vota P, Toia G, Clementi MC, et al. Prostate cancer microvascular routes: exploration and measurement strategies. Life (Basel) 2023;13:2034.
[54] Butler MB, Papageorgiou G, Kanoulas ED, Voulgaridou V, Wijkstra H, Mischi M, et al. Mapping of prostate cancer microvascular patterns using super-resolution ultrasound imaging. Eur Radiol Exp 2025;9:25.
[55] Zhao YZ, Li QY, Zhao P, Yang YH, Jiang B, Luo YK. Feasibility of ultrasound super-resolution microscopy in the differential diagnosis of diffuse prostate cancer. Chin J Med Imag 2026;34:865-869. (in Chinese).
[56] Yang W, Qiu C, Zhai J, Zhang W, Huang C, Shao J, et al. Ultrasound-targeted microbubble destruction mediates PDE5i/NO integration for cavernosum remodeling and penile rehabilitation. Bioeng Transl Med 2023;8:e10568.
[57] Bodard S, Denis L, Pradier B, Chabouh G, Hélénon O, Correas JM, et al. Clinical translation of ultrasound localization microscopy: a narrative review of current applications and future directions. Ultrasound Med Biol 2026;52:891-907.
[58] Xia S, Zheng Y, Hua Q, Wen J, Luo X, Yan J, et al. Super-resolution ultrasound and microvasculomics: a consensus statement. Eur Radiol 2024;34:7503-7513.

清華大學出版社 Tsinghua University Press | SciOpen